# High-quality quantum point contacts in GaN/AlGaN heterostructures

H. T. Chou, S. Lüscher, D. Goldhaber-Gordon, M. J. Manfra, A. M. Sergent et al.

## Additional information on Appl. Phys. Lett.

# High-quality quantum point contacts in GaN/AlGaN heterostructures

H. T. Chou
*Department of Applied Physics, Stanford University, Stanford, California 94305*

S. Lüscher and D. Goldhaber-Gordon[a)]
*Department of Physics, Stanford University, Stanford, California 94305*

M. J. Manfra, A. M. Sergent, and K. W. West
*Bell Laboratories, Lucent Technologies, Murray Hill, New Jersey 07974*

R. J. Molnar
*MIT Lincoln Laboratory, Lexington, Massachusetts 02420-0122*

We study the transport properties of quantum point contacts in a GaN/AlGaN heterostructure. The conductance of our devices shows well-quantized plateaus, which spin-split in high perpendicular magnetic field. The g factor is 2.55, as derived from the point contact subband splitting versus perpendicular magnetic field. In addition to the well-resolved plateaus, we also observe evidence of "0.7 structure" which has been mainly investigated in the GaAs system. © *2005 American Institute of Physics*. [DOI: 10.1063/1.1862339]

Nanofabrication techniques enable researchers to confine electrons in semiconductors to mesoscopic structures. Almost all experiments on mesoscopic semiconductor systems have been based on GaAs/AlGaAs heterostructures. Reasons include clean interfaces with good lattice match, and mature growth and processing technologies developed over more than 30 years.

GaN, with a much larger band gap, has drawn recent interest in industry for use in blue laser diodes and microwave power field-effect transistors. For physics studies, GaN/AlGaN heterostructures are attractive for their high mobility, $\mu=75\,000$ cm$^2$/Vs at 4.2 K,[1] and because of several important differences compared to GaAs. First, no modulation doping is needed: the reduced symmetry of the crystal structure induces a spontaneous polarization, and the lattice mismatch between GaN and AlGaN induces a piezoelectric polarization; the combination of these two polarizations causes a two-dimensional electron gas to accumulate at the interface.[2] Avoiding doping removes one major source of scattering. Second, the higher effective mass (0.2 compared to 0.067)[3,4] and lower dielectric constant (9 compared to 13) in GaN make electron–electron interactions more important. Third, the larger g-factor (2 compared to −0.44)[4] makes it easier to manipulate electron spins with magnetic fields. In principle, a modified layer structure could eliminate spin-orbit coupling[5] so that spins could be transported microns or further without precessing.

In this letter, we report low-temperature studies of gated nanostructures on a GaN/AlGaN heterostructure. Quantum point contacts (QPCs) show quantized conductance plateaus, among the cleanest ever seen outside GaAs. They also display the "0.7 structure,"[6] which has been seen mainly in GaAs QPCs, but also in other semiconductor systems.[7]

A QPC is a narrow constriction between two electron reservoirs. The width of the constriction can be tuned to pass one or more channels of electrons, each with a quantized conductance of $2e^2/h$.[8] Yet as a QPC is just being opened up, its conductance pauses around 0.7 times $2e^2/h$ before rising to the first full-channel plateau.

The 0.7 structure has been one of the prime puzzles in mesoscopic physics since 1996.[6] The shoulder in conductance near $0.7(2e^2/h)$ rises as temperature is lowered below 1 K, merging into the first quantized plateau. It is generally agreed that the 0.7 structure is due to electron interactions. The dimensionless interaction strength $r_s$ has the form $r_s \propto m_e^*/\varepsilon n_s^{1/2}$ where $\varepsilon$ is the dielectric constant, $m_e^*$ is the effective mass and $n_s$ is the electron density. In GaAs QPCs, $r_s$ has been tuned by controlling electron density to study the effect of interactions on 0.7 structure.[9] Interaction strength can also be changed by moving to a different material system, with different dielectric constant and effective mass.

The GaN heterostructure used in this work has a lower dielectric constant and higher effective mass, but also a higher electron density ($n_s=1.0\times10^{12}$ cm$^{-2}$) than a typical GaAs heterostructure. The dimensionless interaction strength $r_s$ is 70% higher than that of the low density ($n_s=1.5\times10^{11}$ cm$^{-2}$) GaAs heterostructures that have been previously used to study 0.7 structure.

The devices measured in this experiment are fabricated on a GaN/AlGaN heterostructure with a 2DEG formed 19 nm below the surface. At 4.2 K, the 2DEG has a density $n_s=1.0\times10^{12}$ cm$^{-2}$ and mobility $\mu=56\,000$ cm$^2$/Vs. Figure 1(a) shows the layer structure, similar to that of Ref. 1. Ti/Al metal pads were annealed to contact the 2DEG. Next, a mesa was patterned by photolithography followed by a Cl-based plasma etch. The split-gate structure that forms the QPC was realized by electron beam lithography followed by evaporation and liftoff of Ni gates [Fig. 1(b)]. The low temperature differential conductance $dI/dV_{sd}$ was measured at 300 mK using a lock-in technique, with a 20 $\mu$V, 77 Hz excitation added to a variable dc voltage $V_{sd}$ applied between source and drain. In each measurement, a magnetic field-dependent series resistance between 3200 and 4000 $\Omega$ was subtracted; taking this series resistance into account aligns conductance plateaus with the expected quantized conductances.

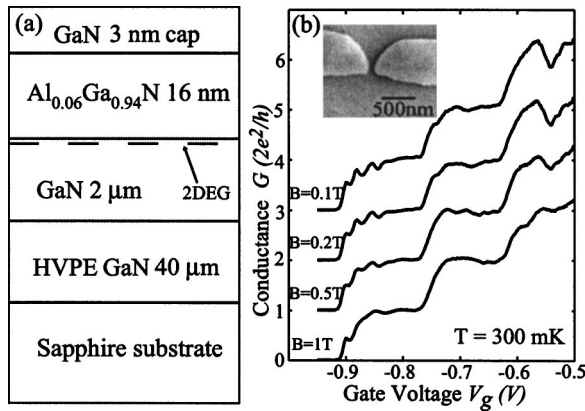[a)]Electronic mail: hungtao@stanford.edu

FIG. 1. (a) Schematic layer structure of the heterostructure. (b) improvement of plateau quantization with the application of a small magnetic field. Linear conductance $G(V_g)$ is plotted at magnetic field $B=0.1$ T, 0.2 T, 0.5 T, and 1 T. Traces are shifted vertically for clarity. Inset: micrograph of the QPC. The gap between the two split gates is 80 nm at its narrowest point. All experimental data shown in this letter were measured at 300 mK.

Near zero magnetic field, the linear conductance $G \equiv dI/dV_{sd}$ ($V_{sd}=0$) of the QPC shows two clear quantized plateaus at $2e^2/h$ and $4e^2/h$. The third and fourth plateaus are obscured by resonances which might be caused by backscattering from defects: the mean free path in our system is only 700 nm, comparable to the largest features of the split-gate structure. A small perpendicular magnetic field improves the quantization of the plateaus. In Fig. 1(b) several resonances periodic in gate voltage are evident at $B=0.1$ T. As the magnetic field is increased to 1 T, the third plateau appears clearly and the resonances are suppressed as backscattering is reduced by the perpendicular magnetic field.

Nonlinear transport measurements can be used to extract subband energies; in addition, the presence of a zero-bias anomaly (ZBA) suggests that electron–electron interactions play an important role in transport through the QPC [Figs. 2(a) and 2(b)]. At low magnetic field [$B=1$ T, Fig. 2(a)], the plateaus in linear conductance appear as a collapsing of traces for different gate voltages at multiples of $2e^2/h$ conductance. For high source-drain bias an extra plateau appears at $0.7(2e^2/h)$. This extra plateau is a characteristic feature of the 0.7 structure in GaAs QPCs. The ZBA below the $2e^2/h$ plateau has also been observed previously in GaAs QPCs, and has been associated with a Kondo-like correlated state that may provide a global framework for understanding the 0.7 structure.[10] At a higher magnetic field [$B=6$ T, Fig. 2(b)], the extra plateau at $0.7(2e^2/h)$ remains at finite bias, but the ZBA is suppressed and linear conductance is quantized in units of $e^2/h=0.5(2e^2/h)$ due to the large Zeeman energy—again, this agrees with observations of GaAs QPCs.

Subband energy spacing is an important parameter of a QPC, determining the temperature and bias voltage ranges over which conductance is quantized. To measure this value, the transconductance ($\partial^2 I/\partial V_{sd}\partial V_g$) is plotted as a function of $V_{sd}$ and gate voltage $V_g$ [Figs. 2(c) and 2(d)]. The peaks in transconductance represent the steps between the conductance plateaus. The dashed lines follow the transconductance peaks as a function of applied bias. The diamond region inside the dashed lines is the $2e^2/h$ plateau. The dashed lines cross at finite bias when the source is aligned to one subband and the drain is aligned to an adjacent subband. Therefore the crossing reveals the subband energy spacing $E=eV_{sd}$, which is 2.7 meV between the $2e^2/h$ and $4e^2/h$ subbands at
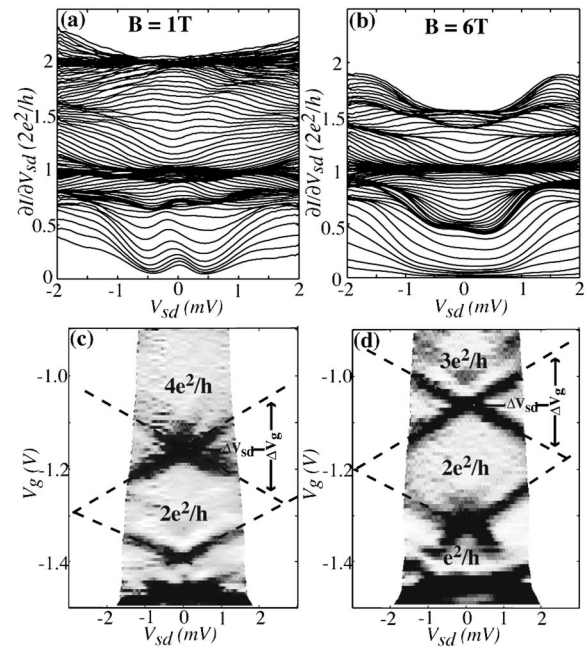


FIG. 2. (a) Nonlinear differential conductance $\partial I/\partial V_{sd}(V_{sd}, V_g)$ at $B=1$ T. One split gate voltage is fixed at $-0.4$ V and the other gate voltage is stepped from $-0.9$ V to $-1.5$ V. The $V_g$ interval between traces is 4 mV. Plateaus in $G(V_g)$ appear as collapsing of traces at $2e^2/h$ and $4e^2/h$ around zero bias. Below $2e^2/h$ a zero bias anomaly (ZBA) appears and at high bias an extra plateau emerges at $0.7(2e^2/h)$; (b) nonlinear conductance at $B=6$ T. Spin-split plateaus appear as collapsing of traces at multiples of $e^2/h$. The extra plateau is suppressed but the extra plateau at high bias remains; (c) numerical derivative transconductance ($\partial^2 I/\partial V_{sd}\partial V_g$) at $B=1$ T. The plotted $V_{sd}$ across the QPC has been corrected to account for the series resistance. Light regions (low transconductance) represent the plateaus and dark regions (high transconductance) represent interplateau steps. The transconductance peak at zero bias splits into an upward peak and a downward peak at finite bias (dashed lines). The difference of the lines' slopes, $\eta=\Delta V_{sd}/\Delta V_g$ $=9.3$ $\mu$V/mV, represents how the gate voltage shifts the 1D subband energy of the QPC; (d) transconductance ($\partial^2 I/\partial V_{sd}\partial V_g$) at $B=6$ T. The diamond inside the dashed line represents the $2e^2/h$ plateau. $\eta=9.4$ $\mu$V/mV is nearly unchanged from the value at $B=1$ T.

$B=1$ T. The splitting of the transconductance peak is linear with $V_{sd}$, indicating that the gate voltage affects the subband energies linearly. Therefore, we derive a coefficient for conversion between gate voltage and energy: $\eta=9.3$ $\mu$eV/mV [see Fig. 2(c)].

A strong magnetic field induces a large Zeeman energy difference ($g^*\mu_B B$) between spin up and spin down subbands. This energy difference results in conductance quantized in units of $e^2/h$ rather than $2e^2/h$. Figure 3(a) shows the linear conductance $G(V_g)$ at four different perpendicular magnetic fields. In addition to its effect on spin in a QPC, a perpendicular magnetic field changes subband energies by adding an extra effective lateral confinement. This does not alter the 1D nature of transport in our QPCs, and does not further discriminate between different spin states. Each quantized plateau simply becomes longer in higher magnetic field because of the larger subband energy. At $B=1$ T, three conductance plateaus quantized in units of $2e^2/h$ are observed, and a shoulder emerges below the first plateau. At $B=4$ T, spin–split plateaus ($e^2/h, 3e^2/h, 5e^2/h$) have already formed, and they are more pronounced at $B=6$ T. The spin–split plateaus are mainly due to the spin–split subbands of QPC at high magnetic field. Though our magnetic field is perpendicular rather than parallel to the 2DEG, the 2DEG reservoir is in the Shubnikov–de Haas regime, not the Quantum Hall
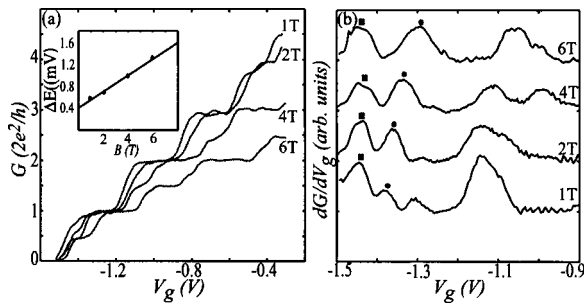
FIG. 3. (a) Linear conductance $G(V_g)$ at perpendicular magnetic field $B$ =1 T, 2 T, 4 T, and 6 T. Spin-split plateaus at multiples of $e^2/h$ start to appear at $B$=4 T; (b) transconductance $(\partial^2 I/\partial V_{sd}\partial V_g)$ from the data in (a). The traces are shifted for ease of comparison. The two peaks denoted by filled square and filled circle are the transitions from 0 to $e^2/h$ and from $e^2/h$ to $2e^2/h$. (a) Inset: energy splitting between first and second spin–split subbands at different magnetic fields. The energy is the product of the peak gate voltage difference from (b) and $\eta$ from Fig. 2(c). The dashed line is a least-squares fit to the data.



FIG. 4. (a) Nonlinear conductance at $B$=1 T shows clear ZBA. The fixed gate voltage is changed to −1 V to obtain fewer resonances. The other split-gate voltage is swept from −0.66 V to −0.84 V. The $V_g$ interval between traces is 4 mV; (b) peak width of the ZBA in (a) vs gate voltage, determined as half the distance between the local minima on the left and the right side. The width increases rapidly from 0.4 mV as the conductance passes $0.7(2e^2/h)$.

regime. Therefore, the spin–split Landau levels of the 2DEG are highly broadened and should only have a minor contribution to the spin–split plateaus.

To deduce the Zeeman energy splitting and calculate the effective $g$-factor $g^*$, we employ the technique developed by Patel *et al.* for GaAs QPCs.[11] In order to get the transconductance, we take the data from Fig. 3(a) and differentiate numerically [Fig. 3(b)]. The first two peaks in Fig. 3(b) originate from steps between conductance plateaus: $0-e^2/h$ and $e^2/h-2e^2/h$. These two peaks occur when the spin up or spin down subband, respectively, is aligned to the Fermi level of the source or drain. These two peaks gradually move apart as the magnetic field increases to 6 T. The energy gap between the spin–split subbands derived from these data is linear in $B$ but with an enhanced splitting at the lowest field 1 T [Fig. 3(a) inset]. A linear fit yields $g^*$=2.55±0.05 and a zero-field offset of 0.395±0.07 meV. Earlier measurements of Shubnikov–de Haas oscillations in a GaN 2DEG yielded a constant $g^*$=2.06 up to a magnetic field of 5 T.[4] Therefore our observed enhancement of the $g$ factor in GaN QPCs is probably due to electron–electron interactions inside the QPCs, not to exchange effects in the 2DEG at high fields. Enhancement of the $g$ factor and a zero field offset in subband splitting were also observed as aspects of 0.7 structure in GaAs QPCs in a parallel magnetic field measurement.[6]

To further investigate the 0.7 structure in our QPCs, the channel was shifted left and right by applying different voltages to the two split gates. The voltage difference was adjusted to find the condition for which resonances were least pronounced. Nonlinear transport measured under this condition [Fig. 4(a)] shows a more profound ZBA below the $2e^2/h$ plateau. The width of the ZBA in Fig. 4(a) is shown in Fig. 4(b). The peak width is 0.4 meV below $G \sim 0.7(2e^2/h)$ and increases rapidly as $G$ approaches $2e^2/h$. We note that this peak width below $G \sim 0.7(2e^2/h)$ is roughly the same as the zero-field offset derived from the inset of Fig. 2(a), although no theoretical connection between these two quantities has yet been established. In GaAs, the width of a similar ZBA above $G \sim 0.7(2e^2/h)$ has been related to the Kondo temperature of an electron trapped in the QPC.[10]
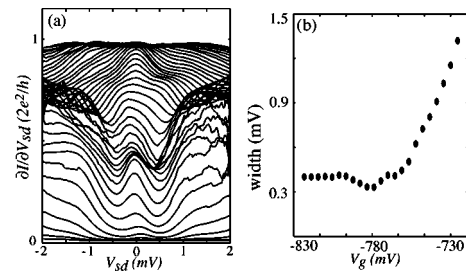
In conclusion, we have fabricated quantum point contacts on a GaN/AlGaN heterostructure using the split-gate technique. The conductance shows well-quantized plateaus at multiples of $2e^2/h$ at low magnetic field. These plateaus split into multiples of $e^2/h$ at high magnetic field. The effective $g$ factor is 2.55, as derived from the subband energy splitting at different magnetic fields. In addition, the imperfectly understood 0.7 structure in GaAs/AlGaAs QPCs is also observed in our GaN/AlGaN QPC. This observation suggests strong electron–electron interaction in our device even at high 2DEG density, consistent with the high effective mass of electrons in GaN. Future experiments to measure the effects of temperature, 2DEG density, and QPC shape may improve our understanding of 0.7 structure in GaN as well as in other semiconductor systems.

[1]M. J. Manfra *et al.*, J. Appl. Phys. **92**, 338 (2002).
[2]O. Ambacher *et al.*, J. Appl. Phys. **85**, 3222 (1999).
[3]S. Syed, J. B. Heroux, Y. J. Wang, M. J. Manfra, R. J. Molnar, and H. L. Stormer, Appl. Phys. Lett. **83**, 4553 (2003).
[4]W. Knap, E. Frayssinet, M. L. Sadowski, C. Skierbiszewski, D. Maude, V. Falko, M. Asif Khan, and M. S. Shur, Appl. Phys. Lett. **75**, 3156 (1999).
[5]J. P. Lu, J. B. Yau, S. P. Shukla, M. Shayegan, L. Wissinger, U. Rossler, and R. Winkler, Phys. Rev. Lett. **81**, 1282 (1998).
[6]K. J. Thomas, J. T. Nicholls, M. Y. Simmons, M. Pepper, D. R. Mace, and D. A. Ritchie, Phys. Rev. Lett. **77**, 135 (1996).
[7]P. Ramvall *et al.*, Appl. Phys. Lett. **71**, 918 (1997).
[8]B. J. van Wees, H. van Houten, C. W. J. Beenakker, J. G. Williamson, L. P. Kouwenhoven, D. van der Marel, and C. T. Foxon, Phys. Rev. Lett. **60**, 848 (1988).
[9]K. S. Pyshkin, C. J. B. Ford, R. H. Harrel, M. Pepper, E. H. Linfield, and D. A. Ritchie, Phys. Rev. B **62**, 15842 (2000).
[10]S. M. Cronenwett, H. J. Lynch, D. Goldhaber-Gordon, L. P. Kouwenhoven, C. M. Marcus, K. Hirose, N. S. Wingreen, and V. Umansky, Phys. Rev. Lett. **88**, 226805 (2002).
[11]N. K. Patel, J. T. Nicholls, L. Martin-Moreno, M. Pepper, J. E. F. Frost, D. A. Ritchie, and G. A. C. Jones, Phys. Rev. B **44**, 13549 (1991).